Port Isolation Method for MIMO Antenna in Small Terminals for Next Generation Mobile Networks

Tatomirescu, Alexandru; Pelosi, Mauro; Knudsen, Mikael B.; Franek, Ondrej; Pedersen, Gert Frølund

Link to publication from Aalborg University

Port Isolation Method for MIMO Antenna in Small Terminals for Next Generation Mobile Networks

Alexandru Tatomirescu*, Mauro Pelosi*, Mikael B. Knudsen†, Ondrej Franek*, Gert F. Pedersen*

*Section of Antennas, Propagation and Radio Networking (APNet),
Department of Electronic Systems, Faculty of Engineering and Science, Aalborg University,
DK-9220 Aalborg, Denmark {alext, mp, of, gfp}@es.aau.dk
†Intel Mobile Communications, DK 9220 Aalborg, Denmark mikael.knudsen@intel.com

Abstract—**This paper presents a practical method to increase the isolation between two ports of a Multiple Input Multiple Output (MIMO) antenna for mobile hand-held devices. The method consists in a connecting strip containing lumped components placed in between the low impedance zones of the two antennas. The lumped components modify the impedance of the connecting strip so that, together with the mutual coupling impedance, it acts as a band-stop filter between the two ports.**

As a consequence, the efficiency due to scattering parameters almost doubles and the envelope correlation coefficient decreases dramatically. Furthermore, the use of lumped components makes this method less susceptible to the presence of other components in the mobile device or the user. This method has been verified on two antenna configurations, through simulation and measurements.

I. Introduction

In recent years, the need for higher data rate has increased greatly. Users want to access applications that are more demanding on the current mobile data networks, such as online music or film and low latency internet. The 4th Generation (4G) proposes to satisfy this need. MIMO systems offer increased data rate and robustness by using spatial multiplexing [1]. The size of a modern hand-held device is small compared to the wavelength used in some of the 4G communication systems like the 700 MHz for Long Term Evolution (LTE) band which is chosen by the operators for the increased coverage capabilities. Consequently, it becomes an issue when MIMO is introduced because of the antennas' mutual coupling. The coupling increases due to the fact that the antennas are electrically close, as shown in [2]. The capacity and efficiency are considerably decreased by the poor isolation between the antennas [3],[2].

Solutions for reducing the coupling at frequencies higher than 2 GHz have been analyzed and proposed in [4], [5] and [6], all of which are solutions for a specific type of antenna. For the lower bands, LTE 700 and 800, the ground plane of a typical bar-type mobile phone is less than $\lambda/10$ wide and $\lambda/5$ long, and the spacing of the antennas is between $\lambda/50$ and $\lambda/10$, which results in a high mutual coupling. The authors of [7] present the use of metamaterials to limit the currents on the ground plane, thus reducing the high coupling at these low frequencies. In [8], a hybrid coupler with lumped components is used, while in [9], a connecting strip between the antennas is implemented to solve the same problem using the principle

shown in [4].

This paper improves the solution used in [4] and proposes the use of lumped components for the isolation mechanism. It has been evaluated on two antenna configurations.

II. Simulation setup

The first antenna design used in this paper is shown in figure 1. It has been simulated with the Finite Difference Time Domain (FDTD) method with a cell size of 0.5 mm. It consists of two meander-line monopoles printed on a support that has the relative permittivity of 4.4 and conductivity of 0.004 S/m at 1 GHz. The size of the antenna is 52x25x0.05 mm^3. The total Printed Circuit Board (PCB) is standard FR4 of 52x110x1 mm^3. The antennas have a simple design chosen for operation in the LTE lower band. The same specifications were used in manufacturing a prototype and measurements have been done with the network-analyzer.
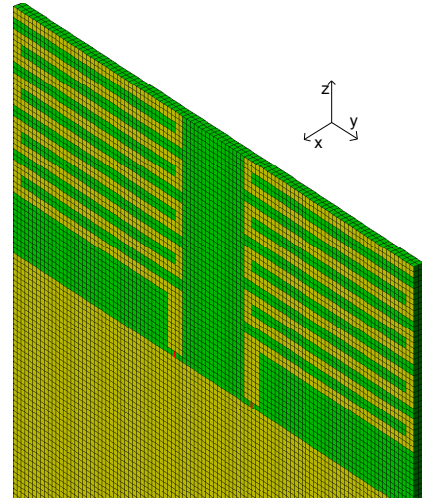

Fig. 1.   The simulated antenna 1 where the red lines represent the feed port and the cell size is 0.5 mm.

The second antenna, shown in figure 2, has been simulated using FDTD with a cell size of 0.5 mm. It consists of two monopole antennas folded on a support that has the relative permittivity of 2.3 and size of 40x20x5 mm^3. The total Printed Circuit Board (PCB) is standard FR4 of 40x100x1 mm^3. The antennas have been designed to have multiple band

operation including the LTE lower band. A prototype with these specifications has been manufactured for measurements.
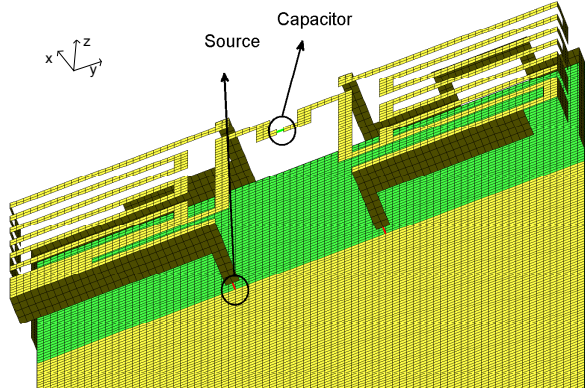

Fig. 2. The simulated antenna 2. The antenna support is invisible in this figure. Cell size 0.5 mm.

III. DISCUSSIONS AND RESULTS

An evaluation of the performance of a MIMO antenna must contain an analysis of efficiency, near-field coupling, as well as envelope correlation.

The near-field coupling is evaluated through the S_{21} parameter, which is a measure of the power dissipated in the load of the second antenna when one is excited. This affects drastically the efficiency and the envelope correlation coefficient of the signal at the antenna's ports.

The total efficiency is calculated based on the antenna's S-parameters using equation 1 [2], where η_{rad} is the radiation efficiency that takes into account conductive and dielectric losses. Following [10], the envelope correlation coefficient can be calculated knowing the far-field radiation pattern by using equation 2. For the receiving scenario, this equation is valid only when uniform three-dimensional (3-D) angular power spectrum of the received signal is assumed.

$$\eta_{total1} = \eta_{rad1} * (1 - |S_{11}|^2 - |S_{21}|^2) \qquad (1)$$

$$\rho_e = \frac{|\int_0^\pi \int_0^{2\pi} [\overrightarrow{F}_1(\theta,\phi) \bullet \overrightarrow{F}_2]d\phi \sin\theta d\theta|^2}{\int_0^\pi \int_0^{2\pi} |\overrightarrow{F}_1(\theta,\phi)|^2 d\phi \sin\theta d\theta \int_0^\pi \int_0^{2\pi} |\overrightarrow{F}_2(\theta,\phi)|^2 d\phi \sin\theta d\theta} \qquad (2)$$

where $\bullet$ denotes the Hermitian product and $\overrightarrow{F}_i(\theta,\phi)$ is the radiation pattern when port i is excited.

The following subsections describe the implementation and results of the decoupling method proposed in [4], which consists of a strip connected between the antennas.

A. Antenna 1

The antenna in figure 1 has the simulated frequency response plotted in figure 3. A strong coupling between the two antennas can be seen. It has been shown in [4] that it

is possible to counteract this undesirable phenomenon by a connecting strip that is inserted between the antennas, close to the feeding point, in the low impedance area of the antenna, as shown in figure 4. Simulations results show that the coupling is reduced considerably for a narrow bandwidth of approximately 20 MHz at -10 dB.
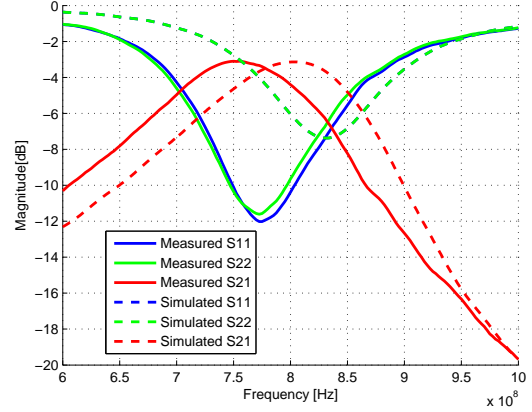

Fig. 3. The simulated and measured S parameters of the antenna 1.

Neutralizing the mutual coupling between elements of an antenna array is not a new subject for research. The authors of [11] show that a necessary condition for canceling the mutual coupling is a purely imaginary transadmittance of the array at the desired frequency ($real(Y_{21}) = 0$). In figure 4 is plotted the transadmittance of the antenna 1 and the susceptance in the case with the two antenna's feed ports connected through a strip containing a 10 nH inductor (in parallel with the antenna). In the latter case, the coupling is neutralized at 750 MHz. By changing the transadmittance, the antenna's input impedance is also modified. Therefore, a matching network is needed to obtain matching at the decoupled frequency. Through a parametric study, the position of the connecting strip can be chosen in such a way that the remanding part of the antenna (from the connecting port to the feed points) can act as a matching network.

The variation of the length, shape and width of the connecting strip has proven that for some antenna geometries, independently of the strip's design, the connecting strip does not offer isolation in the band of interest. If the needed susceptance cannot be obtained just by using the strip, a lumped component can be used to modify the impedance of the connecting strip, thus changing the decoupling frequency. In the case with a capacitive coupling ($imag(Y_{21}) < 0$), a connecting strip that acts as a parallel inductance is needed. The combined effect of the two is similar to the one of a band-stop filter between the two antennas, at any required frequency. For an inductive coupling ($imag(Y_{21}) > 0$), a capacitive strip must be used, as shown in subsection III-B.

Consequently, for antenna 1, an inductor has been connected between the two antennas instead of a longer meandered strip, as in figure 5. Through simulation the optimal value of the
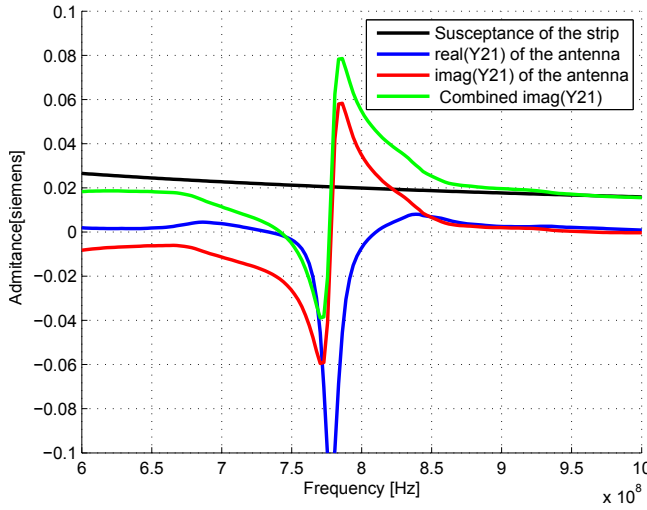
Fig. 4.   Transadmittance of antenna 1, the strip and the combined effect.

Fig. 6.   The simulated S parameters of the antenna with the connecting strip and an inductor, antenna 1a from figure 5. S11 is identical to S22 due to symmetry.

inductor, 10 nH, has been obtained and the simulated results are shown in figure 6. Antenna 1a presents both decoupling and matching for a bandwidth of 20 MHz around 855 MHz. There is a shift in resonating frequency because the radiating part of the antenna is smaller by one meandering which has been used as a matching network.
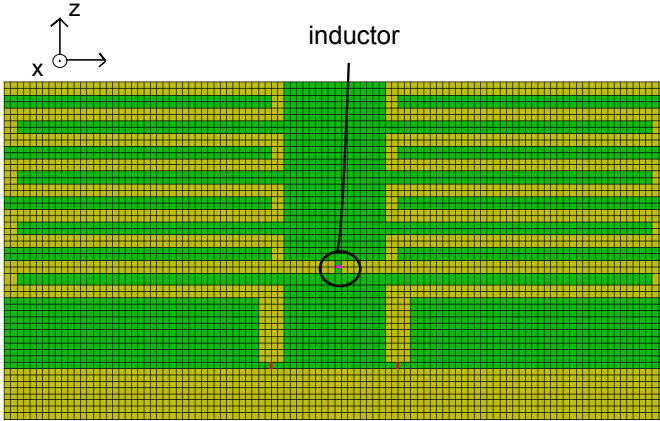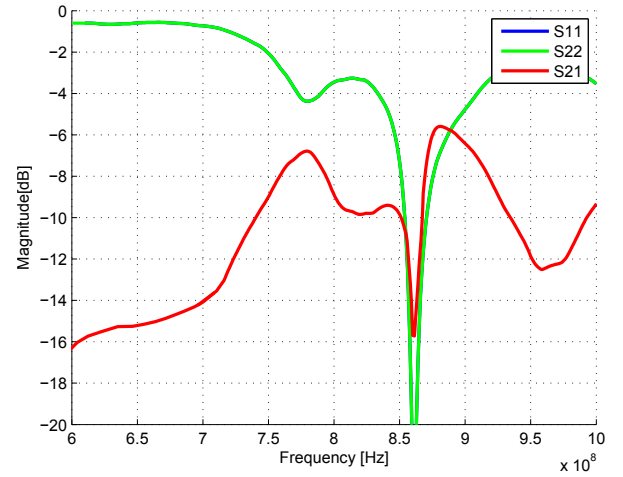

Fig. 5.   The decoupling strip containing a lumped iductor represented by the magenta line, antenna 1a.

Based on these simulations, a prototype has been constructed and measured. It has a wire-winded surface mounted 10 nH coil with tolerance of 10% and a quality factor (Q) of 58. The results plotted in figure 7 were obtained from measurements in agreement with the simulated results. The difference between them is due to the fact that the FDTD algorithm makes some approximations. In addition, the interactions of the measuring setup with the antenna have not been simulated.

The total efficiency for the antennas connected with a inductor has been measured in the anechoic chamber at the frequency of 828 MHz for one antenna and it is -4 dB due to considerable losses in the FR4 material(2.6 dB from
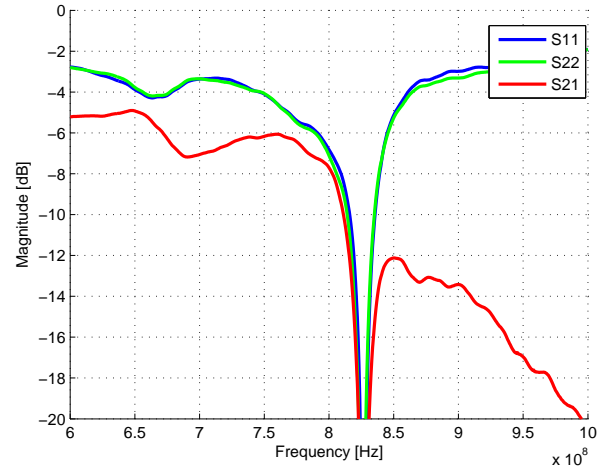

Fig. 7.   The measured S parameters for the prototype of the antenna 1b from figure 5.

measurements) and also in the inductor, although it has a high Q. From equation 1, the scattering efficiency can be calculated for the whole measured band by neglecting the radiation losses. Compared to the case with no decoupling mechanism, a considerable improvement in efficiency can be seen, as shown in figure 8.

By using equation 2 and the far-field radiation patterns, the envelope correlation coefficient can be obtained. With the simulated radiation patterns of the two antennas at 860 MHz, for the case with a connecting strip and an inductor, a ρ_e of 0.01 is obtained whereas at 834 MHz, in the case without, a ρ_e of 0.56 is obtained. By using the measured S parameters and the approximation given in [12], the envelope correlation coefficient can be calculated. It is plotted in figure 9.
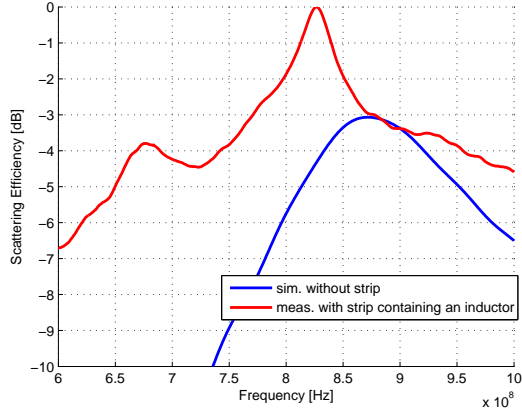
3

Fig. 8. The calculated scattering efficiency for the antenna configuration with and without decoupling strip, antenna 1a respectively antenna 1, when the radiation losses are neglected.
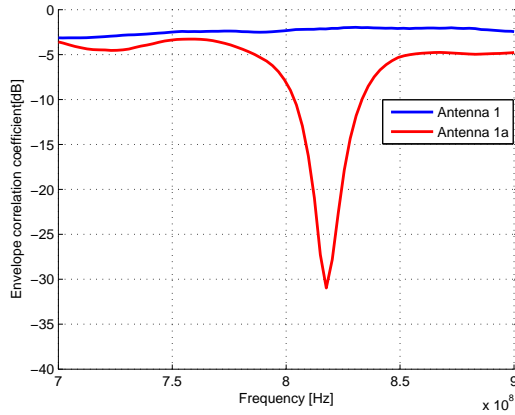

Fig. 9. Calculated envelope correlation coefficient for the measured S parameters.
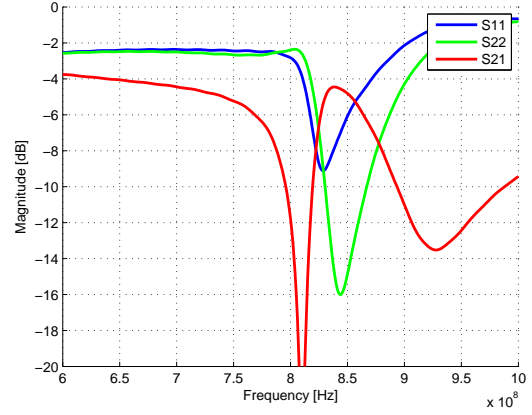

Fig. 10. The simulated S parameters of the antenna 2a that has no capacitor.

the antennas have no connecting strip. Simulated envelope correlation coefficient is 0.03 and 0.81 without the connecting strip. Just by varying the shape of the connecting strip, finding
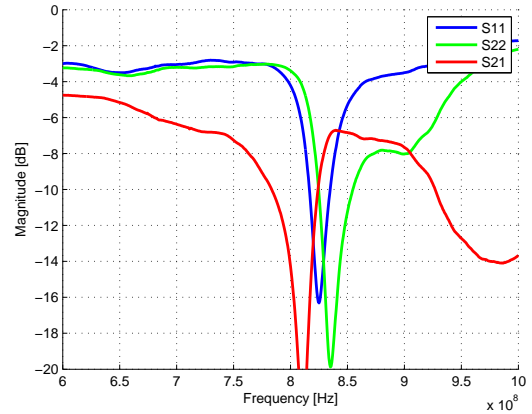

Fig. 11. The measured S parameters of the antenna 2a.

B. Antenna 2

The second antenna presented in this paper is a multiple band antenna, similar to the one used in [9]. It has been chosen to replicate the results obtained for the first one, on a more complex antenna design.

The simulation results of the antenna from figure 2, without a capacitor (just a simple connecting strip, antenna 2a, which is not shown) are plotted in figure 10. They show that the matching and decoupling frequency band are not the same and measurements confirm this. In figure 11 are plotted the measured scattering parameters of the antenna with a simple connecting strip in the band of interest. The antennas are matched at lower frequencies, around 600 MHz, because the impedance seen is not of the radiation element but is the impedance of the antenna part that connects the two ports terminated with the 50 Ω load. Therefore, a high coupling is present.

The total efficiency at 830 MHz is 0.41 measured and 0.47 simulated, compared to 0.29 in the simulated case when

the required configuration in order to obtain both matching and decoupling can be difficult and, for some designs, unobtainable due to size limitation.

A simpler way of modifying and controlling the decoupling mechanism of the connecting strip is to insert lumped components into the strip, as shown above. Simulated scattering parameters of the antenna from figure 2 are shown in figure 12. The connecting strip contains a 2.25 pF capacitor and the measured response of the prototype antenna, plotted in figure 13, agrees with the simulation. The measured total efficiency for one of the antennas, in the case with a capacitor, is 0.57.

For the simulated gain patterns of the antenna with the connecting strip containing a capacitor, represented in figure 14, the envelope correlation coefficient is 0.02. Furthermore, it can be seen that by using the connecting strip the antennas have orthogonal radiation modes. An effect similar to beamforming can be noticed because both radiating elements are excited by one port.
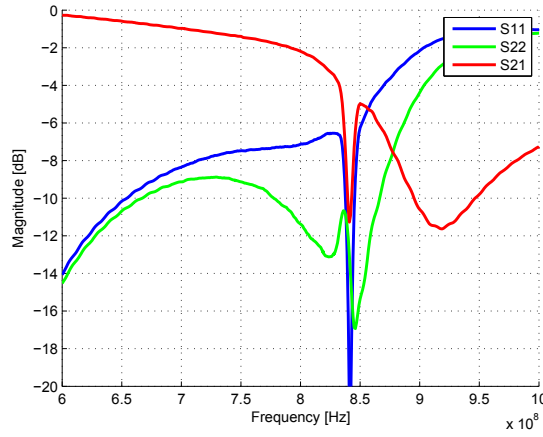
Fig. 12. The simulated S parameters of the antenna 2, the case with the capacitor.
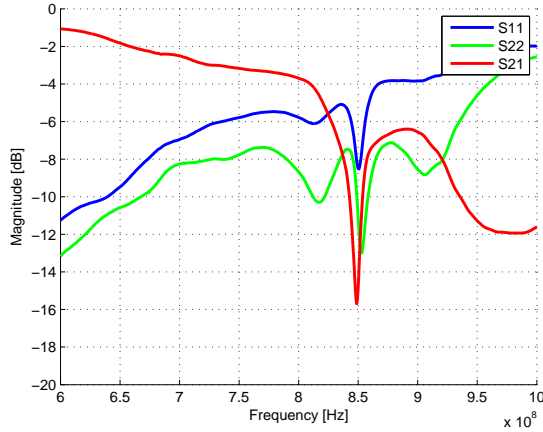

Fig. 13. The measured S parameters of the antenna 2, the case with the capacitor.

Both efficiency and signal correlation have been improved considerably in comparison with the results of the antenna array with no decoupling mechanism. The multiband performances have not been spoiled because the capacitor is behaving like a continuous strip at higher frequencies. The results are not shown for the sake of brevity.

IV. CONCLUSIONS

The implementation of LTE in mobile headsets for commercial applications requires a decoupling mechanism to increase efficiency and isolation between different antenna ports. A connecting strip between the antennas can be used as a decoupling structure. Both performance parameters are greatly improved, making this method a viable candidate for a real implementation.

Lumped components and strip lines can be used instead of simple meandered strip line, thus eliminating the size restrains for the connecting strip. Because the coupling impedance is fixed, a capacitor or an inductor is necessary when the strip is more or less inductive then needed in order to act like a band-stop filter in the band of interest.
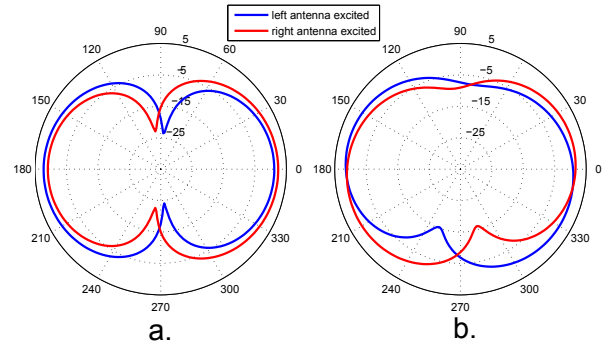

Fig. 14. The simulated radiation patterns in dB at 842 MHz in the Y-Z plane for each of the antennas in the case with no connecting strip at all(a.) and with strip plus capacitor, antenna 2 (b.).

Although the structure of the second antenna presented in this paper seems complex and difficult to implement in practice, the proposed decoupling mechanism improves performance and, by using lumped components, it can be virtually applied to any antenna, not to mention that it facilitates the design procedure. In addition, it has the potential to decouple fixed structure antennas at different frequencies through variable circuit components.

REFERENCES

[1] G.J. Foschini and M.J. Gans, "On Limits of Wireless Communications in a Fading Environment when Using Multiple Antennas", Wireless Personal Communications 6: 311-335, 1998.
[2] B. Lau, J. B. Andersen, G. Kristensson and A. F. Molisch, "Impact of Matching Network on Bandwidth of Compact Antenna Arrays", Antennas and Propagation, IEEE Transactions on, November 2006, VOL. 54, NO. 11.
[3] J. Wallace and M. Jensen, "Mutual Coupling in MIMO Wireless Systems: A Rigorous Network Theory Analysis", Wireless Communications, IEEE Transactions on , VOL. 3, NO. 4, july 2004.
[4] A. Diallo, C. Luxey, P. Le Thuc, R. Staraj and G. Kossiavas, "Study and Reduction of the Mutual Coupling Between Two Mobile Phone PIFAs Operating in the DCS1800 and UMTS Bands", Antennas and Propagation, IEEE Transactions on, VOL. 54, NO. 11,november 2006.
[5] D. Heberling, Ch. Oikonomopoulos-Zachos, "Multiport Antennas for MIMO-Systems", Loughborough Antennas and Propagation Conference, 2009.
[6] L. Liu, R. Langley, "Frequency-Tunable Mobile Phone Antennas with Matching Circuits", Antennas and Propagation (EuCAP), april 2010.
[7] N. Lopez, C. Lee, A. Gummalla and M. Achour, "Compact Metamaterial Antenna Array for Long Term Evolution (LTE) Handset Application", Antenna Technology, 2009. iWAT 2009. IEEE International Workshop on.
[8] R. Bhatti, S. Yi, and S. Park, "Compact Antenna Array With Port Decoupling for LTE-Standardized Mobile Phones", Antennas and Wireless Propagation Letters, IEEE, VOL. 8, 2009
[9] G. Park, M. Kim, T. Yang, J. Byun and A.S Kim , "The compact quad-band mobile handset antenna for the LTE700 MIMO application", Antennas and Propagation Society International Symposium, IEEE 2009. APSURSI '09.
[10] R.G Vaughn, J.B Andersen, "Antenna Diversity in Mobile Communications", Vehicular Technology, IEEE Transactions on, VOL. VT-36. NO. 1, november 1987.
[11] J.B Andersen, H. Rasmussen, "Decoupling and descattering networks for antennas", Antennas and Propagation, IEEE Transactions on, VOL. VT-24. NO. 6, november 1976.
[12] S.Blanch, J. Romeu, I. Corbella, "Exact representation of antenna system diversity performance from input parameter description", Electronics Letters,VOL. 39. NO. 9, May 2003.